WIND- AND BUOYANCY-DRIVEN INTERMEDIATE LAYER CIRCULATION IN THE SEA OF OKHOTSK

Mitsudera H.[1], Matsuda J.[1,2], Nakamura T.[1], Uchimoto K.[1] AND Ebuchi N.[1]

[1]. *Institute of Low Temperature Science, Hokkaido University, Japan*

[2]. *Graduate School of Earth Environmental Science, Hokkaodo University, Japan*

1.INTRODUCTION

The densest water forming in the North Pacific region originates in the northwestern shelf of the Sea of Okhotsk (SO). This water is called the Dense Shelf Water (DSW), produced when cold and salty brine is rejected as sea ice forms (Shcherbina et al., 2004). DSW can be heaved up to about 27.0 σ_θ, so that it is heavy enough to be ventilated below the pycnocline as it flows out from the shelf. Then, DSW is transported along the Sakhalin coast through the intermediate layer of a depth of about 200m to 400m. When it reaches straits along the Kuril Islands in the southern SO, it experiences strong tidal mixing, forming a low potential volticity (PV) water, and is exported out further to the Pacific Ocean; it finally becomes a source of the North Pacific Intermediate Water (Yasuda, 1997).

The ventilation of DSW, the intermediate circulation, and the tidal mixing along the Kuril Islands are also likely to compose a meridional overturning circulation in SO. Recently, Nakamura et al. (2006) focused on effects of the tidal mixing on the SO overturning circulation. In a series of numerical experiments they found that high salinity water entrained from the intermediate layer to the surface layer by the tidal mixing is essential to close the overturning circulation. That is, the entrained saline water is advected northward by the surface circulation in SO and pre-conditions the wintertime DSW formation over the northern shelf. Contrarily, DSW would not be produced if the tidal mixing were absent so that no saline water were entrained in the surface layer.

DSW carries vast materials entraining bottom sediments on the shelf including iron (Nakatsuka et al., 2002; Nakatsuka et al., 2004). Therefore, it is important to simulate DSW and its variability in order to elucidate the 'intermediate layer iron hypothesis' how iron concentration in the surface layer of the western North Pacific Ocean and SO is determined and how it impacts on bio-productivity. Although the effects of the tidal mixing along the Kuril Islands have been understood well, it is not yet clear how various other effects, such as wind, ice formation and fresh water flux interplay and impact on the generation and variability of the overturning circulation. In this report, we will describe numerical simulation of the overturning circulation and its sensitivity by varying these effects.

2. MODEL

We used an ice-ocean coupled model based on an OGCM developed at the Center for Climate System Research (Hasumi, 2000). This is a z-coordinate, primitive-equation OGCM

coupled with a 2-categoly elastic-viscous-plastic ice model. Fig. 1 shows the model domain, which spans between 136-166E and 39-65N. Bottom topography is characterized by a shallow northern shelf, a central basin of about 1000m deep, and a deep Kuril basin of a depth of about 3000m, which is connected to the Pacific Ocean through straits along the Kuril Islands. Horizontal grid spacing is 0.5 degree, while 42 levels in vertical. The model is first spun up with the monthly-mean climatological ECMWF wind stress, heat flux and fresh water flux for 20 years, and is then run further for 20 years with various experimental settings. Freshwater from the Amur River is also included, whose flux is 1.5times10^3 m^3/s for April to November and 0 for December to March next year. It should be noted that no restoration was made on the sea surface temperature (SST) and sea surface salinity (SSS) in SO. We put sponge layers for the eastern and southern boundaries of the model domain. The 40th year results of each case were analyzed.

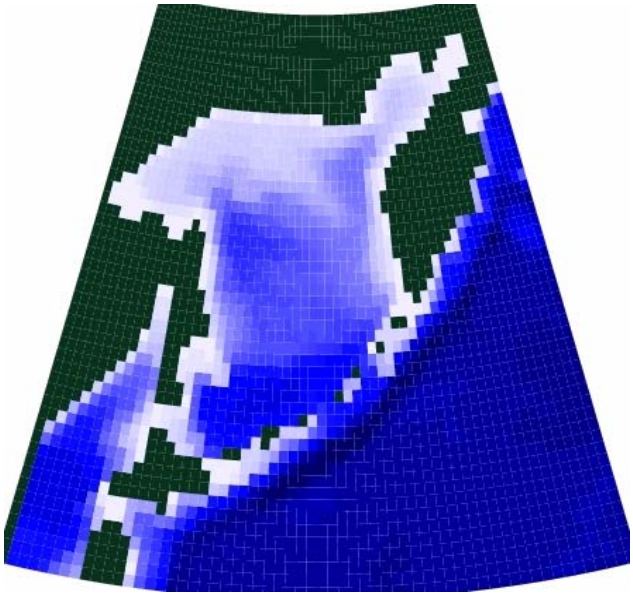

Fig. 1 Model domain and bottom topography

One of driving forces of the overturning circulation is vertical diffusion of heat and salt due to tidal mixing along the Kuril Islands (Nakamura et al., 2006). In order to represent this mixing, we added an enhanced mixing term *Kz** to the vertical mixing coefficient as an ad hoc parameterization (e.g. Nakamura et al., 2006). We used *Kz**=200 cm2/s for a control run because it represents reasonable intermediate layer structures as described in the following sections..

3. OVERVIEW OF MODEL PHENOMENOLOGY

Sea ice distribution is displayed in Fig. 2. The model represents real sea ice features quite well; sea ice tends to cover the entire western basin in March, while there is a relatively large open ocean area in the eastern basin. There are places where ice concentration is smaller than the maximum value of 0,97 along the northern coast in the model, which may be considered as coastal polynyas in this model. Accordingly, salinity flux is large in the northern shelf, which is more than a half of the total production of sea ice in SO.

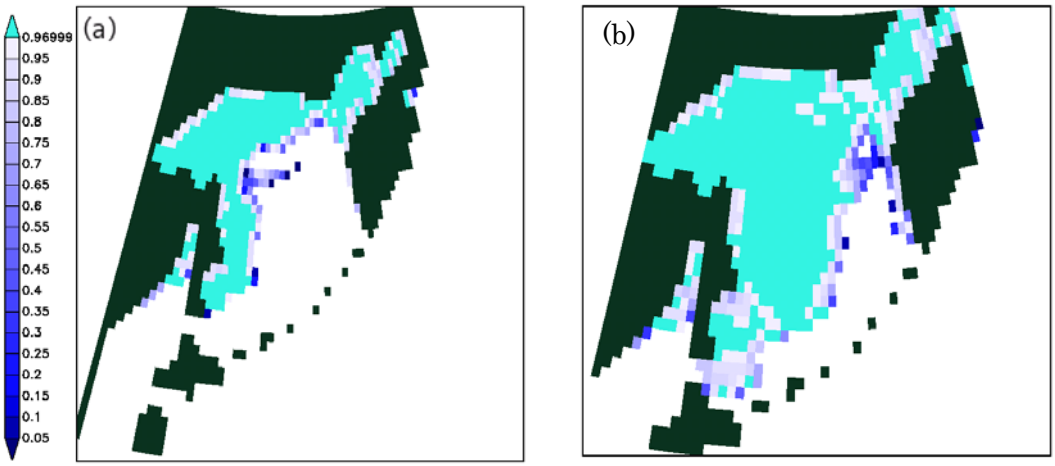

Fig. 2 Simulated sea ice concentration: (a) January, (b) March

An anti-clockwise circulation is generated in the northern and central basin. This is a wind-driven circulation as discussed by Ohshima et al. (2004). The anti-clockwise circulation is stronger in wintertime because of the larger cyclonic wind stress, although its transport is rather small, about 3 Sv. In the southern Kuril basin, a clockwise circulation is generated, which is stronger in summer. The transport is as much as 3 Sv, comparable to that of the northern anti-clockwise circulation. Further, a throughflow of the Soya Strait between the Sakhalin and Hokkaido from the Sea of Japan (the Soya warm current) is linked to the clockwise circulation in summer. This circulation is caused by the enhanced mixing along the Kuril Island.

Fig. 3 displays the potential temperature along the 26.9 sigma theta isopycnal surface in March. This density layer outcrops to the surface over the northern shelf since water denser than 26.9 σ_θ is produced at surface by high salinity flux due to brine rejection. Coldest water below -1.0 degree is found around there. This water is considered as DSW production in this model. DSW dives as deep as 200m along the east coast of Sakhalin as it flows to the south. These features of DSW are consistent with those in Itoh et al. (2003), although it is seen in a somewhat shallower depth than reality.

On the other hand, warm water is present in the southeastern region of SO. This water originates from the western Pacific Ocean through the Kuril straits, being modified by tidal mixing. Its potential temperature is about 2 degree; this is a little warmer than that in Itoh et al. (2003). This water is advected to the north along the eastern shelf by the wind-driven

current. A part of the flow bifurcates to the northwest direction around 52 N, following the bottom topographic contours (see Fig. 1). Further, there is warm and deep circulation (> 400 m) in the southern Kuril basin. This is associated with the clockwise circulation caused by the localized tidal mixing along the Kuril Islands. The feature is also consistent with that in Itoh et al. (2003).

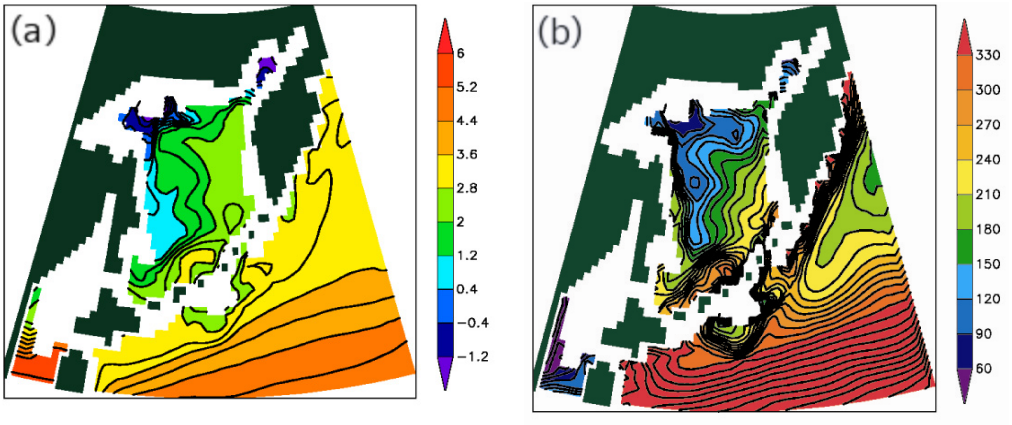

Fig. 3 (a) Potential temperature distribution on 26.9 σ_θ, (b) Depth of the26.9 σ_θ layer.

Since the intermediate layer potential temperature is quite realistic, this case may be considered as a control case in the following experiments. To our knowledge, this is the first simulation of the SO intermediate layer that is comparable to observations.

4. NUMERICAL EXPERIMENTS

4.1. Effects of tidal mixing along the Kuril Islands

This is a similar experiment to those by Nakamura et al. (2006). Four cases were done, besides the control case, with varying the enhanced tidal mixing along the Kuril Islands, where *Kz**=0, 100, 500, 1000 m2s-1; they are referred to as the Tide0, Tide100, Tide500, and Tide1000 cases, respectively. Fig. 4 shows the intermediate-layer potential temperature in September of the five cases including the control case. The potential temperature becomes low as *Kz** increases, consistent with the results by Nakamura et al. (2006). Impacts are particularly evident on the western boundary current off the coast of Sakhalin.

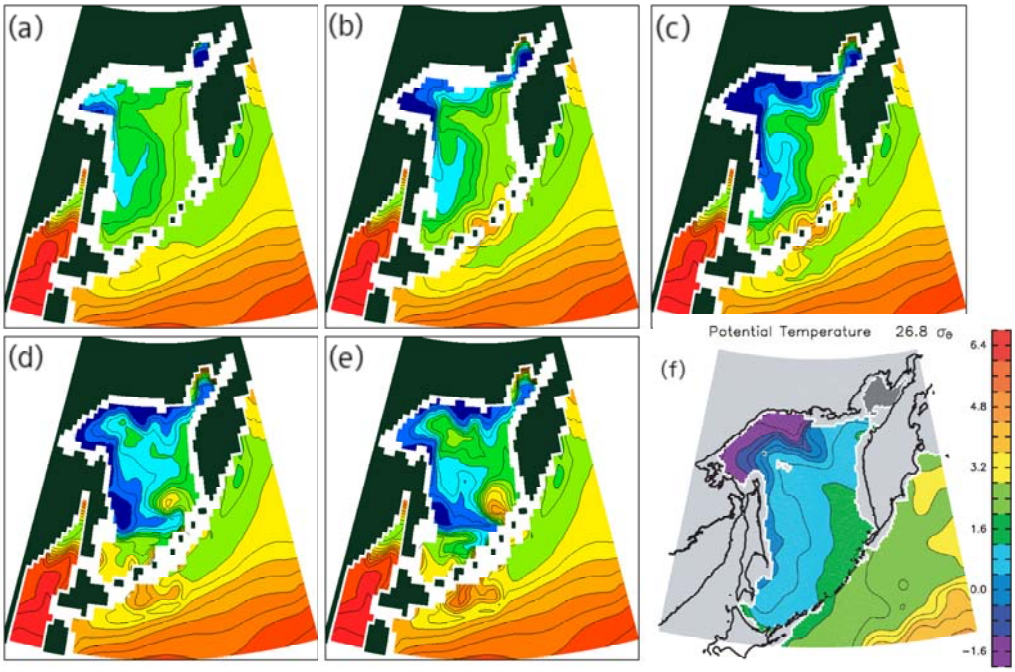

Fig. 4 Potemtial temperature on the 26.8 σθlevel. (a) Tide0 case, (b) Tide100 case, (c) Control case, (d) Tide500 case, (e) Tide1000 case. Observed data by Itoh et al. (2002) is also displayed in (f).

Sea Surface Salinity (SSS) distribution indicates that SSS along the Kuril Islands increases as *Kz** increases. This occurs because a larger amount of deep (hence saline) water upwells there with a larger mixing region. The water in the eastern basin becomes more saline with the *Kz** increase, because the water originates around the Kuril Island is transported northward via surface anti-clockwise circulation. Consequently, the stronger mixing is a cause of saltier water over the northern shelf, resulting in producing heavier DSW. Fig. 5 summarizes relationship between SSS in SO and DSW flux across the 52N section, where DSW here is defined by potential temperature $\theta < -1$ and density rho > 26.6 sigma theta. Clearly, DSW flux increases as SSS, or the mixing along the islands, increases. On the other hand, the ice production does not change significantly among the cases. These results support the conclusion of Nakamura et al. (2006), i.e., the DSW production may increase regardless of ice formation as far as surface salinity increases due to tidal mixing.

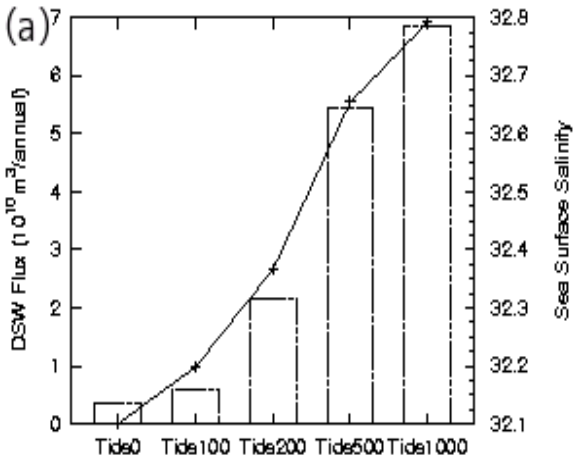

Fig. 5 Solid line with crosses denotes annual mean SSS averaged over the Sea of Okhotsk with various tidal mixing. Histogram denotes the annual DSW flux on the cross section of 53N. Tide200 here corresponds to the control case.

4.2. Effects of winds

It was found that impacts of wind strength on the overturning circulation are significant. Experiments of 4 cases are examined by multiplying factors of 0, 0.5, 1.5 and 2.0 to the control wind stress. These cases are referred to as the Wind0, Wind0.5, Wind1.5 and Wind2.0 cases, respectively. Note that the wind speed to calculate bulk flux formulae is unchanged, so that heat flux is not affected by the changes in wind.

Fig. 6 shows potential temperature distribution in an intermediate layer (26.8 sigma theta). Clearly, potential temperature decreases substantially as wind stress increases. Since the surface circulation is strengthened as wind increases, larger salt flux is transported from the south, leading to higher SSS over the northern shelf for a stronger wind. In Fig. 7, the surface salinity and DSW flux of the various wind cases, together with the Tide1000 case, are displayed. Even though the averaged surface salinity in the Tide1000 case is nearly the same as that in the Wind2.0 case, the DSW flux is much larger in the latter. This indicates that not only the SSS but also the wind-driven circulation itself is important for the DSW flux increase.

We may understand this process in a similar manner to subduction of mixed layer water into thermocline layer, although the flow here is controlled by bottom topography. If a flow passes a polynya where outcropping of a certain density occurs, the water is heaved to be DSW by salt flux due to brine rejection. DSW then subducts below the mixed layer into the intermediate layer, being controlled by topography. DSW finally joins the East Sakhlin Current. Since salinity is continually supplied from the south, SSS is kept high in the shelf region even when the DSW outflow is large. Therefore, salt flux from the shelf is controlled by the flow strength. In conclusion, the DSW flux becomes larger as the circulation becomes stronger, which cools the intermediate layer efficiently with increasing the wind factor.

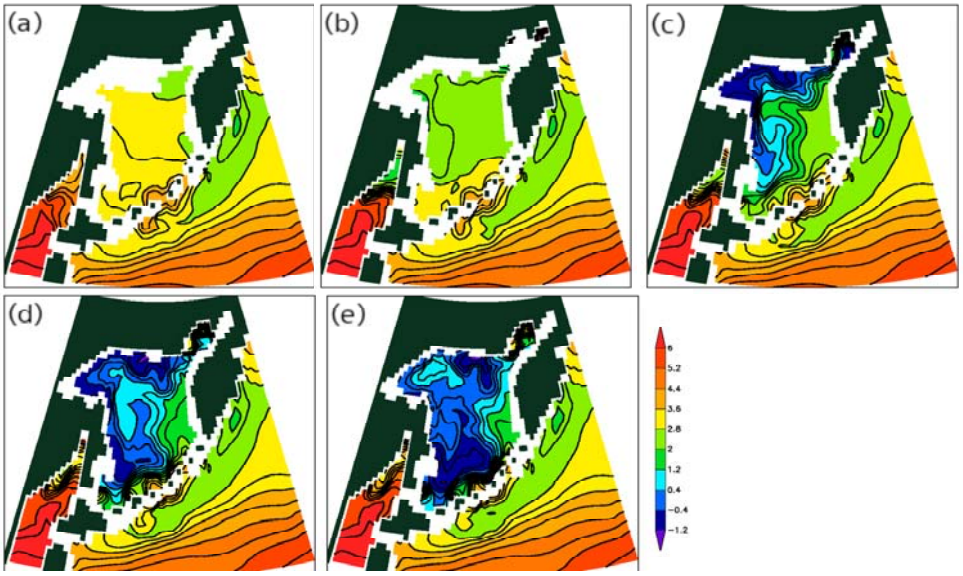

Fig. 6 Intermediate-layer potential temperature with various wind factors. (a) Wind0 case, (b) wind0.5 case, (c) control case, (d) wind1.5, (e)Wind 2.0 case, respectively.

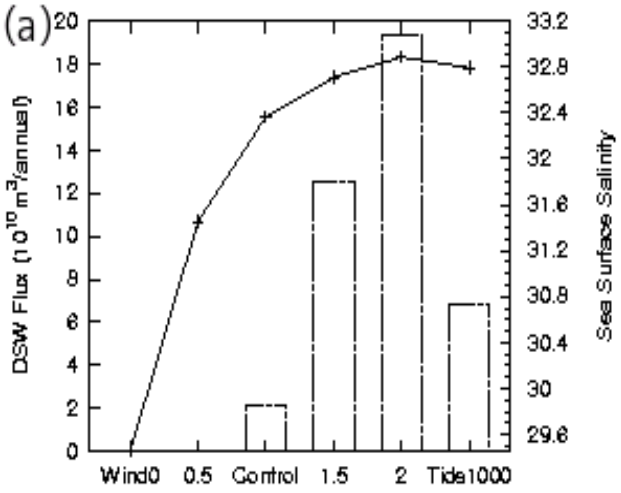

Fig. 7 Same as Fig. 5 except for various wind-factor cases. The Tide1000 case is also displayed.

4.3. Effects of air-temperature increase

In this section, effects of air temperature variations are examined by adding constant air temperature, delta Ta, to the whole region. We made 3 cases of experiments with delta Ta =-3, +3, and +10℃, referred to as the Ta-3, Ta+3, and Ta+10 cases, respectively.

Sea ice coverage is reduced greatly as the air-temperature increases. The Ta-3 case, sea ice covers whole OS region. On the other hand, there are almost free of sea ice with the Ta+10 case. The open water is expanded from the southeastern basin as air-temperature increases, because warm water originating in the North Pacific and around the islands is advected in the eastern basin and prevents SO from being frozen.

The decrease in the ice production causes decrease in DSW formation greatly. This prevents surface water from subducting to the depth of 26.8σ_θ layer, causing the potential temperature increase. In the present study, the intermediate layer temperature rise is as much as +0.6℃ for the Ta+3 case. This is a reasonable rate of rise compared with the results of observed data by Nakanowatari et al. (2007), who showed that temperature trend in the intermediate layer of 26.8-27.0 sigma theta level is +0.6℃ for the last 50 years, when the air-temperature trend along the SO coast is 2.0±1.2℃.

4.4. Impact of the Amur River

DSW may be affected by vast amount of freshwater runoff from the Amur River, because its mouse is located at the northwestern shelf where DSW formation occurs. Surface salinity at the river mouse is less than 30 psu. After the riverine water is exported, it then flows along the eastern coast of Sakhalin toward Hokkaido coast (e.g. Itoh et al., 2003; Uchimoto et al., 2007).

We conducted an experiment in which the Amur River runoff is removed; this is referred to as the Amur0 case. Salinity increases by about 1.0 psu along the Sakhalin coast in March when the river runoff is absent. In summer when the river runoff is included, the difference becomes about 6 psu near the mouse of the river. Salinity in the southern basin also increases by 0.4 psu for the Amur0 case. It is interesting to see, however, that sea ice formation is not affected greatly by the presence or absence of the river runoff. Sea ice can form in the open ocean because the pycnocline between the surface mixed layer and the intermediate layer is strong enough to prevent the surface water from deep convection. Further, over the northern shelf region, sea ice can be produced regardless of salinity because of its shallow depth of the ocean.

Potential temperature in the intermediate layer decreases substantially (about 0.5℃) when the river runoff is switched off. It is found that the DSW is produced along the Sakhalin coast in the Amur0 case, in addition to the DSW production over the northern shelf. This provides the intermediate layer with additional cold water flux. In other words, because of the presence of the Amur River in reality, DSW formation along the Sakhalin coast is limited, and the water is not influential to the intermediate-layer properties even though polynyas can form there.

5. SUMMARY AND DISCUSSION

In this paper we described results of numerical experiments on the overturning circulation in the Sea of Okhotsk (SO), including dense shelf water (DSW) formation and intermediate layer circulation. The numerical results exhibited realistic structures of the circulation. Results may be summarized as follows:

1. The overturning circulation is composed of the ventilation of DSW over the northern shelf, the southward western boundary current in the intermediate-layer, upwelling due to tidal mixing along the Kuril Islands, and northward wind-driven surface current in the eastern basin of SO. These are consistent with those discussed by Nakamura et al. (2006).

2. The DSW flux (defined by $\theta < -1$, $\sigma_\theta > 26.6$) into the intermediate layer, and consequently potential temperature on the layer, is affected strongly by variations in the tidal mixing strength, wind-forcing strength, air-temperature rise and freshwater flux from the Amur River. The experimental results by changing tidal mixing strength support those of Nakamura et al. (2006), i.e., the DSW flux increases as the tidal mixing is strengthened.

3. Intensification of the wind-driven circulation contributes to the DSW flux increase in two ways. One is to give larger salt flux from the Kuril Islands to the northern shelf region via the northward surface current. SSS over the northern shelf increases as wind forcing increases, causing heavier DSW production. The other is to increase export of DSW, or subduction, from the shelf region into the intermediate layer. This makes the potential temperature decrease on the intermediate layer when the wind becomes strong.

4. Atmospheric warming results in intermediate layer warming through decrease in the DSW flux. The intermediate layer warming of +0.6℃ responding to air-temperature increase of +3℃ is a reasonable range compared with those in reality (Nakanowatari et al., 2007).

5. If the fresh water flux from the Amur River is turned off, DSW production along the Sakhalin coast increases greatly.

This is a first simulation that may be comparable to observations of thermohaline structures in the SO intermediate layer. SSS is, however, somewhat large. This gives a large outcropping area of the intermediate density (26.8 $\sigma\theta$, say), implying that larger amount of the intermediate water may be produced. Parameterization of polynyas is one of future subjects.

REFERENCE

Hasumi, H. (2000) CCSR Ocean Component Model (COCO), CCSR Rep. 13, 68pp.,.

Itoh, M., K. I. Ohshima, and M. Wakatsuchi (2003) Distribution and formation of Okhotsk Sea Intermediate Water: An analysis of isopycnal climatology data, Journal of Geophysical Research, 108, 3258, doi: 10.1029/2002JC001590.

Nakamura T., T. Toyoda, Y. Ishikawa, and T. Awaji. (2006) Enhanced ventilation in the Okhotsk Sea through tidal mixing at the Kuril Straits. Deep Sea Research Part I, 53, 425-448, 2006

Nakamura T. and T. Awaji. (2004) Tidally-induced diapycnal mixing in the Kuril Straits and its role in water transformation and transport: A three dimensional nonhydrostatic model experiment. Journal of Geophysical Research, Vol. 109, C09S07, doi: 10.1029/2003JC001850, 2004.

Nakanowatari, T., Kay I. Ohshima, and M. Wakatsuchi (2007) Warming and oxygen decrease of intermediate water in the northwestern North Pacific, originating from the Sea of Okhotsk, 1955-2004, Geophysical Research Letters, 34, L04602, doi: 10.1029/2006GL028243.

Nakatsuka, T., C. Yoshikawa, M. Toda, K. Kawamura, and M. Wakatsuchi (2002) An extremely turbid intermediate water in the Sea of Okhotsk: Implication for the transport of particulate organic matter in a seasonally ice-bound sea. Geophysical Research Letters, 29, 16, 1757, 10.1029/2001GL014029.

Nakatsuka, T., M. Toda, K. Kawamura and M. Wakatsuchi (2004) Dissolved and particulate organic carbon in the Sea of Okhotsk: Transport from continental shelf to ocean interior, J. Geophys. Res. 109(C09S14). doi:10.1029/2003JC001909.

Ohshima, K. I., D. Simizu, M. Itoh, G. Mizuta, Y. Fukamachi, S. C. Riser, and M. Wakatsuchi (2004)

Sverdrup balance and the cyclonic gyre in the Sea of Okhotsk. Journal of Physical Oceanography, 34, 513-525.

Shcherbina, A. Y., L. D. Talley, and D. L. Rudnick (2004) Dense water formation on the northwestern shelf of the Okhotsk Sea: 1. Direct observations of brine rejection,

Journal of Geophysical Research, 109, C09S08, doi:10.1029/2003JC002196,

Uchimoto K., H. Mitsudera, N. Ebuchi, and Y. Miyazawa (2007) Anticyclonic eddy caused by the Soya Warm Current in an Okhotsk OGCM. Journal of Oceanography, 63, 379-391.

Yasuda, I. (1997) The origin of the North Pacific Intermediate Water. Journal of Geophysical Research, 102, 893-909.